Transcription factor p63 controls the reserve status but not the stemness of horizontal basal cells in the olfactory epithelium

Nikolai Schnittke[a,b,c], Daniel B. Herrick[a,b,c], Brian Lin[a,b], Jesse Peterson[a,b], Julie H. Coleman[a,d], Adam I. Packard[a,b], Woochan Jang[a], and James E. Schwob[a,1]

[a]Department of Developmental, Molecular and Chemical Biology, Tufts University School of Medicine, Boston, MA 02111; [b]Program in Cell, Molecular and Developmental Biology, Sackler School of Graduate Biomedical Sciences, Tufts University, Boston, MA 02111; [c]Medical Scientist Training Program, Sackler School of Graduate Biomedical Sciences, Tufts University School of Medicine, Boston, MA 02111; and [d]Program in Neuroscience, Sackler School of Graduate Biomedical Sciences, Tufts University, Boston, MA 02111

Edited by John G. Hildebrand, University of Arizona, Tucson, AZ, and approved July 24, 2015 (received for review June 25, 2015)

Adult tissue stem cells can serve two broad functions: to participate actively in the maintenance and regeneration of a tissue or to wait in reserve and participate only when activated from a dormant state. The adult olfactory epithelium, a site for ongoing, life-long, robust neurogenesis, contains both of these functional stem cell types. Globose basal cells (GBCs) act as the active stem cell population and can give rise to all the differentiated cells found in the normal tissue. Horizontal basal cells (HBCs) act as reserve stem cells and remain dormant unless activated by tissue injury. Here we show that HBC activation following injury by the olfactotoxic gas methyl bromide is coincident with the down-regulation of protein 63 (p63) but anticipates HBC proliferation. Gain- and loss-of-function studies show that this down-regulation of p63 is necessary and sufficient for HBC activation. Moreover, activated HBCs give rise to GBCs that persist for months and continue to act as bona fide stem cells by participating in tissue maintenance and regeneration over the long term. Our analysis provides mechanistic insight into the dynamics between tissue stem cell subtypes and demonstrates that p63 regulates the reserve state but not the stem cell status of HBCs.

reserve stem cell | colony-forming unit | retroviral transduction | neural regeneration | lineage tracing

Stem cells harvested from adult tissues are a promising source of material for use in regenerative medicine if they can be appropriately identified and manipulated. Recent studies in a wide range of adult tissues, including the lining of the gastrointestinal tract, the adult and embryonic CNS, the hematopoietic elements of bone marrow, and the olfactory epithelium (OE), which is the neuroepithelium within the lining of the nasal cavity that subserves odorant transduction, have yielded a somewhat unexpected result: Multiple molecularly and morphologically distinct cell types within a tissue have the capacity to function as stem cells and satisfy even the most stringent criteria of stemness (1–7). Broadly, these populations can be functionally distinguished as active (participating in routine tissue maintenance) and reserve (dormant under normal circumstances but capable of activation by injury to participate in tissue regeneration) (8–10).

The OE provides a unique system to study the dynamics between active and reserve stem cells. The extensive neurogenic and regenerative capacity of the OE in both rodents and humans persists throughout adult life and is unmatched elsewhere in the nervous system (11–14). The two populations of stem cells that are present in the OE fit the active–quiescent dichotomy described above. The active population, globose basal cells (GBCs), constitutes a heterogeneous set of ostensibly lineage-committed and uncommitted progenitor cells that normally persist throughout adult life (6, 15, 16). GBCs are unique to the OE, identifiable at early stages of embryonic development, and are functionally and molecularly homologous to the embryonic olfactory placode progenitor cells (17–19). In contrast, the dormant population, horizontal basal cells (HBCs), which share molecular and morphological similarities with basal cells in other tissues, first appear perinatally at a time when the architecture and cellular constituents of the OE are fully formed (20, 21). HBCs very rarely contribute to cellular maintenance in undamaged tissue, even in the face of accelerated neuronal turnover, but can become activated by severe and direct injury to the epithelium and thereby give rise to all the cellular components of the OE during regeneration (7).

The transcription factor protein 63 (*p63*) is expressed in the basal stem cell populations of stratified epithelia such as the epidermis, and *p63*-knockout mice fail to form stratified epithelia altogether (22, 23). Cell-autonomous, conditional ablation of *p63* causes cell death, senescence, spontaneous differentiation, or robust mitotic amplification depending on the cell type and mutated isoform (24–27). Because of the complexity of the *p63* gene, which encodes six potential isoforms, and the large number of putative target genes, a wide array of functions has been attributed to this transcription factor including the generation, maintenance, self-renewal, proliferation, and differentiation of stem cells as well as both tumor-suppressor and oncogenic roles. Because many of these processes would be mutually exclusive within a given cell population, it is most likely that p63 operates in a highly context-dependent manner as a pivotal switch in a variety of processes

Significance

Harnessing the inherent capability of stem cells to maintain and regenerate injured tissues is a prerequisite for their use in mending damage to the nervous system. In the olfactory epithelium stem cells accomplish neurogenesis and epithelial repair throughout life to an extent not seen elsewhere in the nervous system. Here we show that the transcription factor protein 63 (*p63*) is a master regulator of the transition from the reserve to the active stem cell pool in the epithelium. Loss of *p63* expression in reserve basal cells is necessary and sufficient for activation, without compromising stem cell status. Identification of this central mechanism provides a target for stem cell activation in this uniquely accessible source of patient-specific, neurogenic stem cells.

Author contributions: N.S., D.B.H., B.L., J.P., J.H.C., A.I.P., W.J., and J.E.S. designed research; N.S., D.B.H., B.L., J.P., J.H.C., and W.J. performed research; N.S., D.B.H., B.L., J.P., J.H.C., A.I.P., W.J., and J.E.S. analyzed data; and N.S., D.B.H., B.L., J.P., J.H.C., A.I.P., W.J., and J.E.S. wrote the paper.

The authors declare no conflict of interest.

This article is a PNAS Direct Submission.

[1]To whom correspondence should be addressed. Email: jim.schwob@tufts.edu.

This article contains supporting information online at www.pnas.org/lookup/suppl/doi:10.1073/pnas.1512272112/-/DCSupplemental.

including cell adhesion, cell-cycle regulation, and cell-signaling pathways known to regulate stem cell function.

During embryonic development, olfactory placodal-like progenitors and GBCs express *p63* in the perinatal period before giving rise to HBCs. By adulthood, *p63* (specifically, the isoform lacking the N-terminal *trans*-activation domain, *ΔNp63*) is expressed exclusively in mature HBCs. Genetic knockout of *p63* results in an OE in which HBCs do not differentiate but that appears otherwise normal at the light and electron microscopic level (20). This effect is in stark contrast to the knockout of *p63* in other stratified epithelial tissues, which do not form in mutant animals (22, 23). Moreover, HBC activation following injury is accompanied by p63 down-regulation (20), and conditional knockout (cKO) of *p63* results in the spontaneous differentiation of HBCs (28). In one interpretation of these data, p63 is essential for the self-renewal of the stem cell population in the OE. However, this interpretation does not take into account several features unique to olfactory epithelial maintenance, namely, a subset of GBCs are likely to be stem cells (6, 15), activated HBCs must transition through a GBC stage during regeneration (7), and HBCs are largely dispensable in both the embryonic generation and in the adult maintenance of the OE (7, 20).

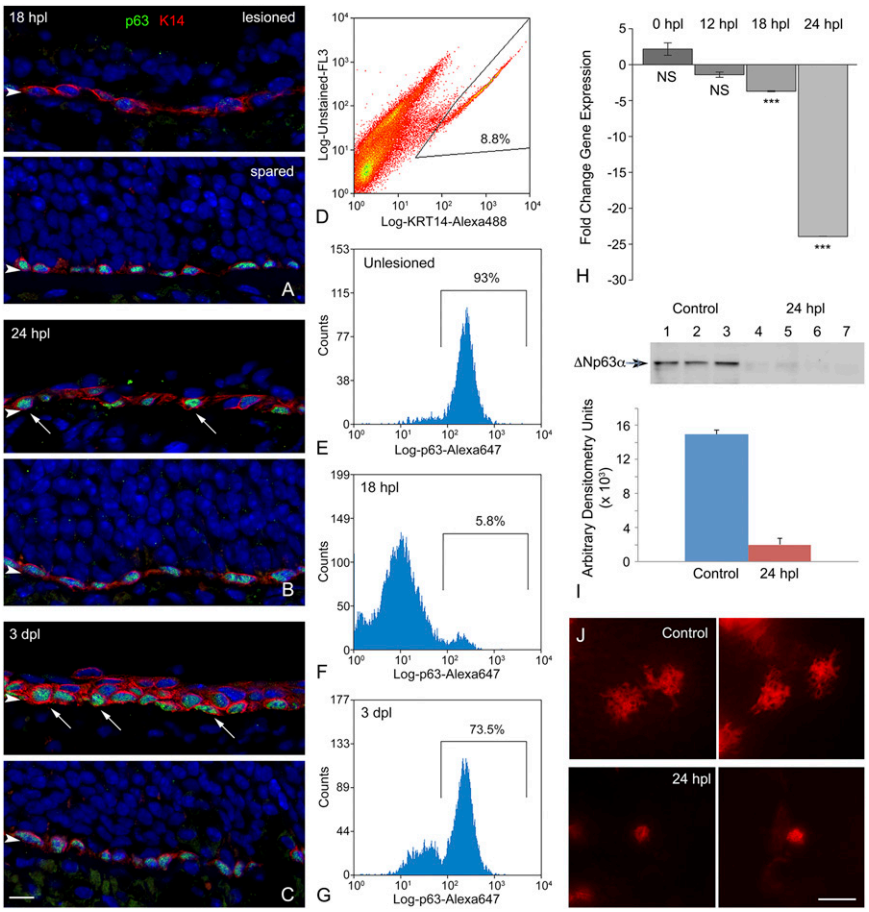

Fig. 1. HBCs respond to MeBr exposure with declines in p63 protein- and gene-expression levels and morphological changes. (*A*–*C*) K14 and p63 staining over an acute time course after unilateral MeBr exposure. The lesioned side is the top image in each pair, and the spared side of the same animal is on the bottom. (*A*) At 18 hpl the mature cells of the OE on the lesioned side have been largely shed, and the $K14^+$ HBCs are still arrayed as a monolayer. However, the level of p63 staining has declined precipitously in all the cells in this field, by comparison with a comparable area on the unlesioned side. (*B*) At 24 hpl, the level of p63 staining on the lesions side has bifurcated. For some $K14^+$ cells, particularly those adjacent to the basal lamina, staining for p63 has rebounded to be indistinguishable from that on the unlesioned side (arrows). (*C*) By 3 dpl, $K14^+$ cells are disposed in multiple layers, with the intensely $p63^+$ cells adjacent to the basal lamina (arrows). (Scale bar: 10 μm for *A*–*C*.) (*D*–*G*) The immunohistochemical pattern observed in *A*–*C* is confirmed when the septal OE is dissected and dissociated and the constituent cells are fixed, jointly stained with anti-K14 and anti-p63 antibodies, sorted on the basis of K14 positivity, and analyzed for p63-staining. (*D*) Example of the sorting strategy highlighting the population of $K14^+$ cells subjected to analysis of p63 staining. (*E*) Unlesioned OE. The overwhelming majority of $K14^+$ cells are strongly stained for p63. (*F*) At 18 hpl, in contrast to the unlesioned OE, the great majority of the $K14^+$ cells are much more weakly stained for p63 and fall below the analytical gate. In addition, the levels of staining are more heterogeneous, extending over two orders of fluorescent intensity. (*G*) At 3 dpl there has been substantial recovery in the percentage of $K14^+$ cells in which p63 staining exceeds the lower end of the analytic gate, although a substantial population is more lightly stained for p63. The FACS pattern fits well with the immunohistochemical analysis. (*H*) Quantitative PCR (qPCR) analysis for *ΔNp63* isoforms as a function of time after the period of MeBr inhalation; 0 hpl signifies animals killed immediately at the end of the 8-h exposure. The fall-off in gene expression slightly lags the precipitous decline in immunohistochemical staining for p63.Statistical comparison with unlesioned control mice by Student's *t* test; $***P < 0.001$; NS, not significant. (*I*, *Upper*) Western blot analysis of p63 protein levels in normal OE (lanes 1–3) vs. 24 hpl (lanes 4–7). The arrowhead designates the position of the unmodified ΔNp63 band, which is markedly reduced at 24 hpl as shown by densitometry analysis of the blots (*Lower*). (*J*) By 24 hpl the HBCs have undergone substantial simplification of their morphology, as shown in CLARITY-prepared whole mounts of *K5.CreER^{T2} > R26R(TdTomato)* mice. In the septal OE of normal mice, the HBCs display elaborate extensions that presumably indicate hemidesmosomal attachments to the basal lamina, based on comparisons with published electron microscopic examinations. After lesion, the cells lose most of the extensions, rendering them simpler in outline. (Scale bar: 20 μm.)

To define the role of p63 in the dynamics of the cellular context in the OE, a more thorough analysis of the transitions between active and reserve stem cells is necessary. Here, we use transplantation, gain and loss of function, and a variety of lesion models in vivo to define the timing and nature of HBC dynamics. Our data demonstrate that p63 preserves the pool of reserve HBCs in the OE but does not maintain stemness per se and also highlight the contribution of the GBC population to long-term epithelial homeostasis.

Results

p63 Down-Regulation Anticipates Proliferation of Activated HBCs. To analyze the role of p63 in the dynamics of HBC activation, we first sought to describe the timeline of p63 protein down-regulation after unilateral exposure to the olfactotoxic gas methyl bromide (MeBr), which causes activation of HBCs (7). By comparing the lesioned side and the unlesioned side, we found that p63 levels are maximally reduced in cytokeratin 5/cytokeratin 14 (K5/K14)-expressing HBCs at 18 h post lesion (hpl) both by immunohistochemistry and flow cytometric analysis (Fig. 1 *A* and *D–F*); it is worth noting that the spread of labeling intensities observed with flow cytometric analysis is broader at 18 hpl than in the unlesioned control (Fig. 1 *E* and *F*). By 24 hpl the $K14^+$ population begins to bifurcate; in a few cells p63 levels have recovered to normal or nearly normal, but in others p63 has disappeared entirely (Fig. 1*B*). The segregation of $K14^+$ cells into two populations of different p63 staining intensities is strikingly pronounced by 3 d post lesion (dpl) (Fig. 1 *C* and *G*). The overall decline in p63 expression over the first 24 hpl also is observed in both quantitative RT-PCR and Western blot assays (Fig. 1 *H* and *I*). The decline in protein levels revealed by immunohistochemistry or by flow cytometry precedes the drop in *p63* transcript level that is revealed by the quantitative RT-PCR analysis. By 24 hpl the drop in p63 expression is associated with a conspicuous simplification of HBC morphology and elimination of the extensive processes that normally characterize them (Fig. 1 *B* and *J*). Down-regulation of p63 occurs significantly earlier than the proliferative burst of HBCs, which previously has been associated with activation (7). $K14^+$ or $CD54^+$ HBCs are first labeled by the expression of Ki67, a marker of active cell cycling, at 24 hpl (Fig. S1 *A–C*), and mitotic rates peak at 3 dpl [phosphohistone H3 (pH3) staining] (Fig. S1 *D–F*). Moreover, both $p63^+$ and $p63^-$ cells are labeled by 5-ethynyl-2'-deoxyuridine (EdU) incorporation with a similar time course after lesion, indicating that the lack of *p63* expression, in and of itself, does not correlate with active cell cycling (Fig. S1 *G–N*).

An in Vivo cfu Assay Identifies Activated HBCs and Correlates with p63 Down-Regulation. We have demonstrated previously that, in contrast to GBCs, HBCs isolated from normal, intact OE do not engraft and do not participate in epitheliopoiesis after transplantation into MeBr-lesioned OE (6). In accordance with the expectation that multipotency after transplantation is a hallmark of active, but not of dormant, stem cells, we transplanted an equal number of labeled HBCs harvested from uninjured mice or mice killed 18 h after MeBr exposure. HBCs were labeled by injecting mice bearing the *K5.CreER^{T2}* driver and the *R26R(TdTomato)* reporter (abbreviated KT) with 300 mg/kg tamoxifen 2 wk before harvesting. Tamoxifen treatment resulted in TdTomato expression in 75 ± 17% of HBCs and their progeny. Because the uninjured OE contains one or more multipotent stem cell populations capable of engrafting and participating in epithelial regeneration, we mixed the KT donor cells with cells from the olfactory mucosa of an unlesioned *β-Actin.GFP* (BACT.GFP) mouse (in which GFP is constitutively expressed by a chicken β-actin/CMV promoter–driven transgene) (6) to serve as a positive control (Fig. S2).

After transplantation of TdTomato-labeled HBCs from unlesioned OE, we observed only 17 ± 4 engrafted clusters per host animal ($n = 3$) (Fig. 2*A*). These clusters were relatively small with an average of 2.2 ± 0.5 cells per cluster (Fig. 2*B*). Of the 52 clusters, 23 (44%) contained only HBCs as identified by morphology and K14 or CD54 staining (Fig. 2 *C* and *E*); 15 clusters (29%) contained only apical supporting cells, as identified by morphology and intense sex-determining region Y-box 2 (*Sox2*) staining (Fig. 2 *C* and *F*); and six clusters (12%) contained basal cells and supporting cells (Fig. 2*C*). Only three clusters (6%) contained neurons, and of those only one cluster (2%) was found to contain olfactory sensory neurons (OSNs) and supporting cells (Fig. 2*C*). These results are in contrast to the BACT.GFP^+ control cells, which engrafted and gave rise to many simple (consisting of one cell type) and complex (containing more than one cell type) clusters (Fig. S3).

The relative paucity of graft-derived clusters following transplantation of HBCs from the intact OE of unlesioned mice stands in marked contrast to the results obtained when labeled HBCs were transplanted from the OE of mice killed 18 hpl. In the latter case, transplant efficiency, as measured by engraftment, exhibited a 30-fold increase, with 585 ± 48 $TdTomato^+$ clusters observed per host animal ($n = 3$) compared with 17 ± 4 clusters per animal from unlesioned HBCs (Fig. 2*A*). The size of these clusters is more than an order of magnitude larger on average than the normal HBC grafts (27.4 ± 8.3 cells per cluster vs. 2.2 ± 0.5 cells per cluster) (Fig. 2*B*). The 18-hpl–derived clusters included simple colonies consisting of only neurons or only supporting cells as well as significantly more complex colonies, which included combinations of neurons, HBCs, GBCs, supporting cells, and/or Bowman's duct/gland cells (D/Gs) ($P < 0.0001$, χ^2 with Yates' correction) (Fig. 2 *C*, *D*, and *G–I*). Thus, activated HBCs can be identified by their ability to engraft and their multipotency coincident with the maximal down-regulation of p63 in HBCs.

Down-Regulation of p63 Is Necessary for HBC Activation. To test the functional significance of p63 down-regulation after injury, we expressed ΔNp63α in the dividing cells of the OE 24 hpl by intranasal infusion of the murine stem cell virus (MSCV)-ΔNp63α-internal ribosome entry site (IRES)-GFP (MIG-p63) retroviral vector to transduce infected cells and their progeny (Fig. 3*A*). At this time point (24 hpl), the majority (81%) of proliferating, $Ki67^+$ cells are $CD54^-$, and they are more superficial and accessible to viruses following intranasal infusion, suggesting that most, but not all, infected cells are $CD54^-$ GBCs (Fig. S4). MIG-p63–transduced progenitor cells gave rise to much smaller clones compared with the MSCV-IRES-GFP (MIG) control (9.3 ± 2.6 vs. 77 ± 8.3 cells per clone, $P < 0.0001$, Mann–Whitney u test = 472.5, two tailed, $n = 3$) (Fig. 3*B*). Of the MIG-p63 clones, 74% were composed of basal cells only. Upon closer examination, we found that all the analyzed basal cells were immunopositive for HBC markers such as K14 and CD54 and were protein gene product 9.5-negative ($PGP9.5^-$) (Fig. 3 *C* and *D*). On the other hand, MIG-transduced clones were heterogeneous and included both simple and complex clones (Fig. 3 *E* and *F*). When all cell types were grouped independently of clone of origin, a similar pattern emerged: MIG-p63–infected clones rarely differentiate into sensory neurons (11% of progeny compared with 65% in MIG-derived cells) or sustentacular (Sus) cells (4% vs. 11%), whereas MIG-transduced clones reflect the full plastic heterogeneity of proliferating cells at 24 hpl, consistent with past data using retroviral lineage tracing after MeBr lesion in rats (Fig. 3*G*) (29). These findings demonstrate that p63 expression inhibits HBC activation and promotes maintenance of an HBC phenotype and/or its adoption by GBCs, indicating that p63 down-regulation is necessary for HBC activation.

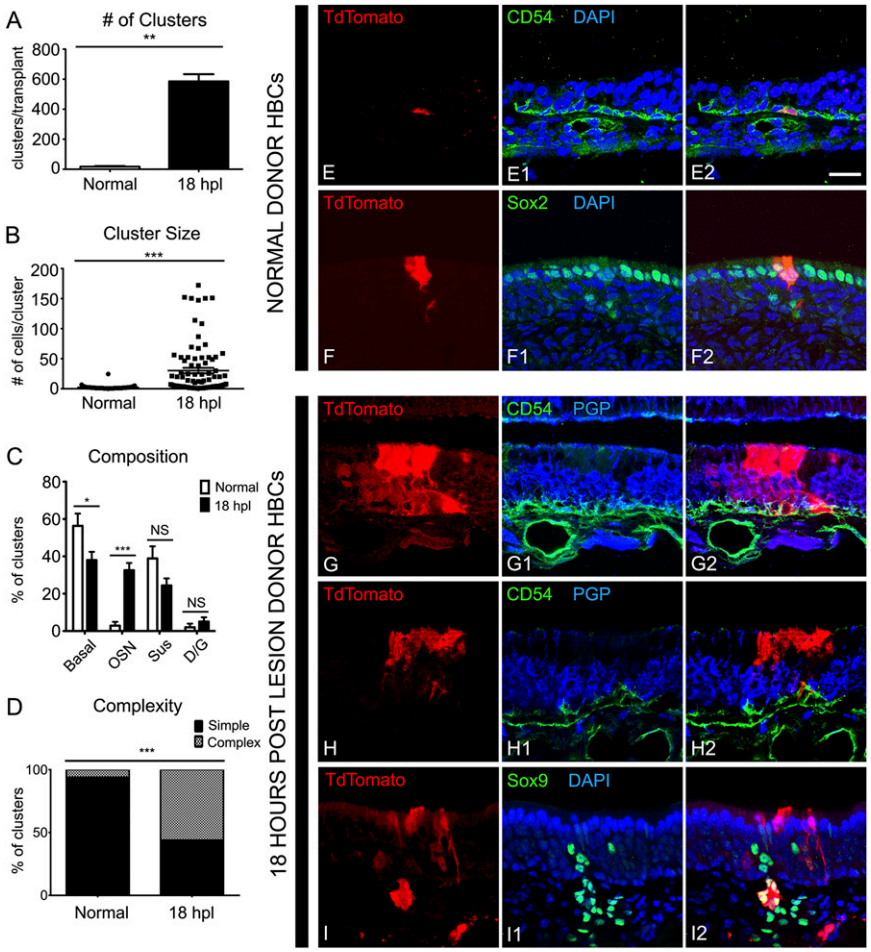

Fig. 2. A cfu assay demonstrates HBC activation at 18 hpl. (*A*) As shown by the number of clusters, HBCs transplanted from HBCs 18 h after MeBr lesion (18 hpl) more efficiently than HBCs from unlesioned donors; $^{**}P < 0.001$, Mann–Whitney test. (*B*) Clusters derived from 18 hpl HBCs are significantly larger than clusters derived from unlesioned donors; $^{***}P < 0.0001$, Mann–Whitney test. (*C*) Summed across all clusters, cells derived from 18 hpl HBCs differentiate into all the mature cell types of the OE including OSNs and Bowman's D/Gs, whereas cells derived from normal HBCs preferentially differentiate into cytokeratin-expressing basal cells and Sus cells; $^{*}P < 0.05$, $^{***}P < 0.0001$; NS, not significant; ANOVA with Bonferroni correction. (*D*) Clusters from 18 hpl HBC are more likely to be complex, containing more than one cell type, than clusters from unlesioned donors; $^{***}P < 0.0001$, χ^2 with Yates' correction performed on raw data. (*E* and *F*) Examples of clusters derived from unlesioned donor HBCs. Unlesioned donors gave rise to predominantly CD54$^+$ HBCs (*E*) and Sox2$^+$ Sus cells (*F*). (*G–I*) Examples of clusters derived from18 hpl donor HBCs. At 18 hpl HBCs gave rise to complex clusters consisting of CD54$^+$ HBCs, PGP9.5$^+$ OSNs, and morphologically distinct Sus cells (*G*), simple clusters consisting of morphologically distinct Sus cells apical to the PGP$^+$ layer of OSNs (*H*), and entire, morphologically distinct, Sox9$^+$ Bowman's D/G units (*I*). (Scale bar: 20 μm.)

Down-Regulation of p63 Is Sufficient for HBC Activation. To determine whether p63 down-regulation is sufficient for HBC activation in the absence of injury, we used mice homozygous for the $p63^{fl/fl}$ allele and bearing the $K5.CreER^{T2}$ driver ($K5.CreER^{T2} > p63^{fl/fl}$) to accomplish cKO of *p63* in HBCs of the unlesioned OE. Recombination events were traced using either LacZ [*R26R(LacZ)*] or TdTomato [*R26R(TdT)*] reporter transgenic strains, depending on technical convenience for immunostaining purposes. In accordance with prior findings (28), we found that 91 ± 2.1% of the reporter-labeled $p63^{fl/fl}$ cells no longer had HBC morphology and were K14$^-$, consistent with HBC activation (Fig. 4 *A–C*). All the labeled $p63^{fl/fl}$ cells that were K14$^+$ (a small minority at 9%) also were immunopositive for p63, indicating incomplete recombination of all three alleles in HBCs following tamoxifen treatment (Fig. 4*I*). Consistent with past studies, the cells that derived from $p63^{fl/fl}$ HBCs included differentiated sensory neurons, GBCs, and rare Sus cells (Fig. 4 *D–H*). We also observed other HBC-derived cells that have not been reported previously. A significant proportion of X-Gal$^+$ cells (2.7 ± 0.9%) were constituents of morphologically identifiable Bowman's D/G units, indicating that HBCs can readily differentiate along this lineage to contribute to Bowman's D/G units in the context of an otherwise unmanipulated OE (Fig. 4*G*). We also investigated the identity of the apical, nonneuronal, X-Gal$^+$ cells, and found that many of them stain positive for the microvillar cell marker TrpM5 (transient receptor potential cation channel, subfamily M, member 5) (Fig. 4*H*). It is noteworthy that the cell types generated following HBC activation include nonneuronal cells, in contrast to the descendants of NeuroD1$^+$ GBCs (29). Thus, it is likely that the persistent GBCs generated by activated HBCs belong to a more upstream GBC subpopulation, such as the Paired box 6 (Pax6)/Sox2$^+$ and/or Ascl1$^+$ cells, which have been shown to be multipotent by retroviral and transplantation analysis (6, 17, 18, 30–32).

Finally, in addition to the findings in the $p63^{fl/fl}$ animals, we found that after tamoxifen administration the incidence of marker-positive/K14$^-$ non-HBCs was significantly higher in $p63^{fl/+}$ animals than in WT $p63^{+/+}$ mice (14.3 ± 3.6% vs. 0.88 ± 0.5%, $P < 0.0001$, Kruskal–Wallis $K = 23.47$, $n = 3$) (Fig. 4*C*). The haploinsufficiency seen with *p63* heterozygosity is further evidence that the effect of

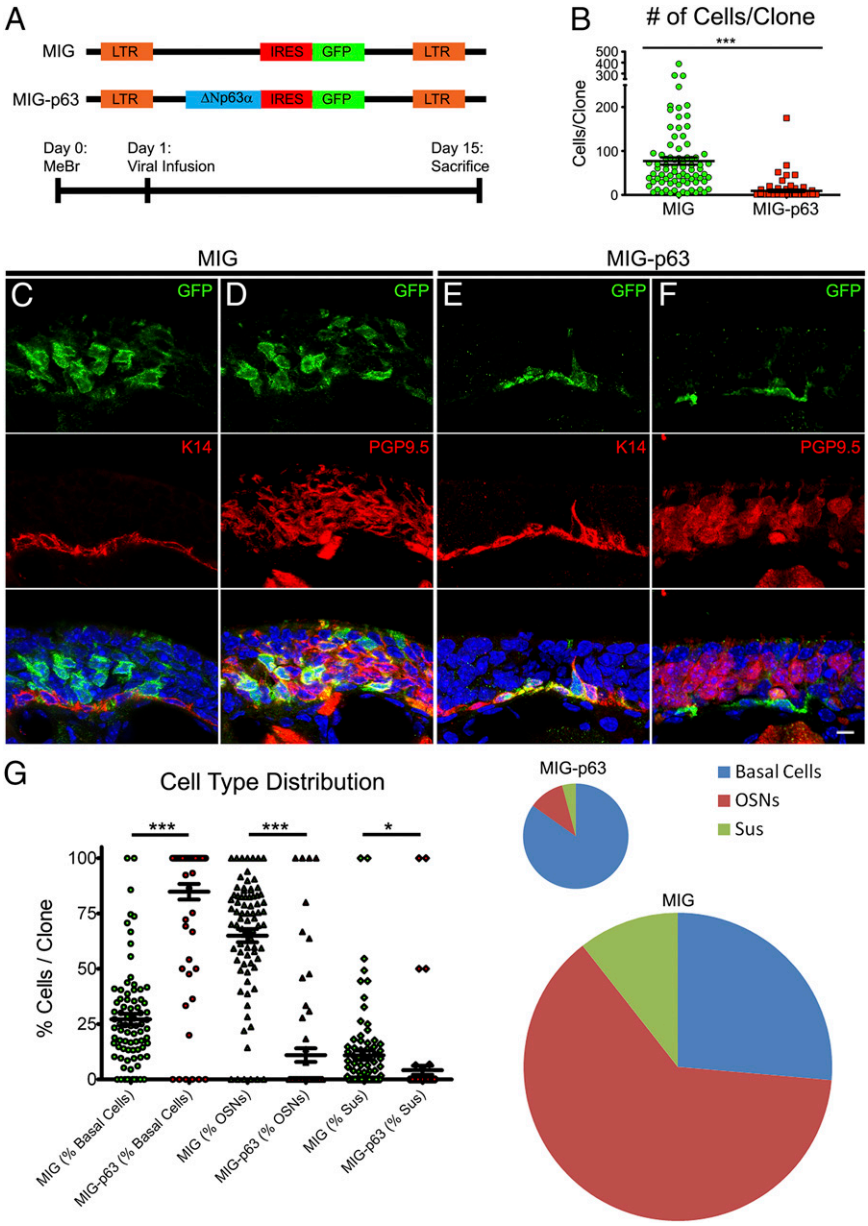

Fig. 3. Down-regulation of p63 is necessary for HBC activation. (*A*, *Upper*) Schematics of retroviral constructs. (*Lower*) Experimental timeline. (*B*) Infection with MIG-p63 significantly attenuated the size of the resultant clones compared with empty vector, MIG-infected controls; ***$P < 0.0001$, Mann–Whitney test. (*C* and *D*) Representative clones resulting from MIG infection. Infection results in large clones including both simple clones, consisting of only one cell type (*C*), and complex clones, consisting of more than one differentiated cell type (*D*). (*E* and *F*) Representative clones resulting from MIG-p63 infection. MIG-p63 infection results in smaller, simple clones consisting of K14$^+$ HBCs (*E*) and, rarely, smaller clones consisting of K14$^+$ HBCs with very few PGP9.5$^+$ OSNs (*F*). (Scale bar: 10 μm.) (*G*, *Left*) Quantitative analysis of cell type distribution by percentage of the contribution of each differentiated cell type to each individual clone. *$P < 0.05$, ***$P < 0.0001$; Kruskal–Wallis test. (*Right*) Pooled data of cell type contribution normalized to average clone size as indicated by pie chart size.

p63 in the OE is dose dependent, as was previously demonstrated in the developing HBCs of the perinatal OE (20). Taken together, the results of *p63* cKO indicate that cell-autonomous loss of p63 is sufficient for HBC activation in a dose-dependent manner even in the absence of tissue injury.

Activated HBCs Give Rise to Persistent, Multipotent GBCs. Past studies have demonstrated that activated HBCs give rise to GBCs when they participate in tissue regeneration, but it is unclear whether the HBC-derived GBCs function as transient progenitors or assume a persistently active stem cell state (7, 28). Published data indicate that GBCs of the normal OE constitute a heterogeneous population, which includes relatively quiescent, long-lived stem cells (GBC_Q), dividing, Sox2/Pax6$^+$ multipotent progenitors (GBC_{MPP}), rapidly dividing transit-amplifying cells (GBC_{TA}), and immediate neuronal progenitors (GBC_{INP}) (17, 18, 31–33). The similarity of the composition of the HBC-derived clones at 4 d and 4 wk after recombination and *p63* deletion suggests that the GBCs function similarly over that time period (Fig. S5).

To analyze the several GBC subtypes, we labeled proliferating GBCs by injecting EdU 2 wk after tamoxifen induction of *K5.CreER^{T2} > p63$^{fl/fl}$;R26R(TdT)* HBCs; a follow-up BrdU pulse was administered 2 h before the animal was killed to label rapidly

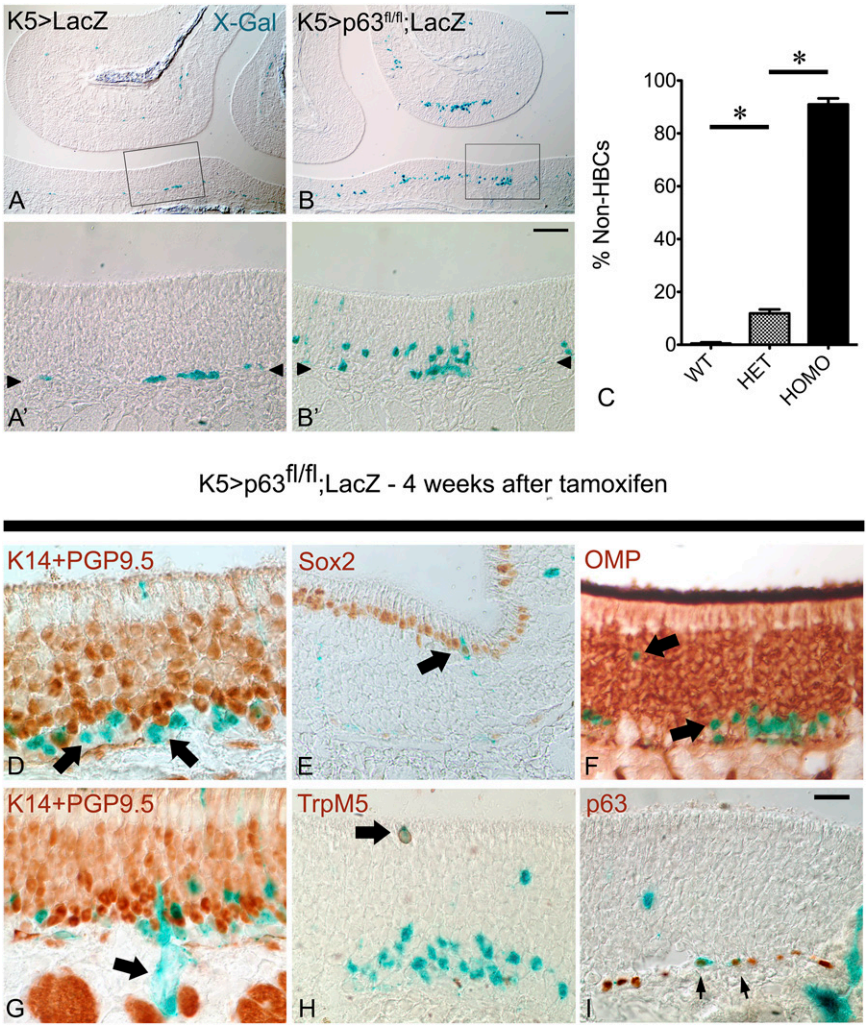

Fig. 4. Down-regulation of p63 is sufficient for HBC activation. (*A* and *B*) Comparison of HBC lineage trace in WT *K5.CreER^{T2} > LacZ* mice (*A* and *A′*) and *p63* cKO in *K5.CreER^{T2} > p63$^{fl/fl}$;R26R(LacZ)* mice (*B* and *B′*) 2 wk after 50 mg/kg tamoxifen induction shows robust HBC activation in cKO vs. WT tissue. (*C*) Quantification of the proportion of non-HBCs derived from K5^{+} cells in WT [*K5.CreER^{T2} > R26R(LacZ)*], heterozygote [HET, *K5.CreER^{T2} > p63$^{fl/+}$;R26R(LacZ)*], and homozygote [HOMO, *K5.CreER^{T2} > p63$^{fl/fl}$;R26R(LacZ)*] tissue, showing a relationship between *p63* gene dosage and activation efficiency; *$P <$ 0.0001; ANOVA with Bonferroni correction. (*D–H*) At 4 wk after tamoxifen (50 mg/kg) administration, HBCs activated by *p63* cKO give rise to all the differentiated cell types of the OE, including K14^{-}/PGP9.5^{-} GBCs situated between the HBC monolayer and the sensory neurons (arrows in *D*); Sox2^{+} columnar Sus cells situated at the apex of the epithelium (arrow in *E*); mature OMP^{+} OSNs (arrows in *F*); Bowman's D/G units (arrow in *G*); and TrpM5^{+} microvillar cells (arrow in *H*). (*I*) In the *K5.CreER^{T2} > p63$^{fl/fl}$;R26R(LacZ)* mice some LacZ^{+} HBCs (identified by their flattened shape) abutting the basal lamina retain expression of p63 protein, indicating that they have not undergone complete recombination of all three alleles. (Scale bars: 50 μm in *A* and *B*; 20 μm in *A′*, *B′*, and *D–I*.)

cycling cells (Fig. 5 *A*, *a*); PGP9.5 labeling was used to identify immature and mature neurons. By operational definition, GBC_{Q}s remained EdU^{+}/BrdU^{-}, whereas GBC_{MPP}s and GBC_{TA}s were double-labeled (EdU^{+}/BrdU^{+}). Finally, the descendants of GBC_{INP}s could be identified as EdU^{+}/PGP9.5^{+} (Fig. 5 *A*, *b*).

We used the above labeling scheme to compare the various categories of GBCs in the GBC population derived from TdTomato^{+} HBCs vs. the population derived from TdTomato^{-} GBCs (which did not differentiate from HBCs activated by excision of *p63*) within the same fields of view. The experiment was performed in four different animals, and 8–12 nonconsecutive sections were analyzed per animal. We found that the majority of both the TdTomato^{-} and TdTomato^{+} (i.e., HBC-derived) GBCs were GBC_{INP}s (64% and 66% respectively); GBC_{Q}s constituted 22% and 19%, respectively, and $GBC_{TA/MPP}$s constituted 14% and 15%, respectively (Fig. 5 *A*, *c* and *d*). These slight differences in distribution were not statistically significant ($P = 0.63$, $\chi^2 = 0.92$), indicating that activated HBCs give rise to GBCs that integrate into the normal OE and function as endogenous GBCs, some of which are persistent, quiescent progenitors.

We next analyzed the functional capacity of HBC-derived GBCs by harvesting and transplanting OE cells from *K5.CreER^{T2} > p63$^{fl/fl}$;R26R (TdTomato)* mice 28 d after tamoxifen administration and HBC activation (Fig. 5 *B*, *a*). At 14 d after transplantation (42 d after activation), there were numerous TdTomato^{+} colonies including neurons, Sus cells, and GBCs, but, as expected, there were no HBCs (Fig. 5 *B*, *b*). The *p63$^{fl/fl}$*-derived clusters also were significantly more complex than the clusters derived from WT HBCs described earlier, with 17 of 71 (24%) clusters containing cells of more than one type, compared with three of 52 (5.5%) ($P < 0.05$, χ^2 with Yates' correction) (Fig. 5 *B*, *c*). The persistence of HBC-derived GBCs indicates that at

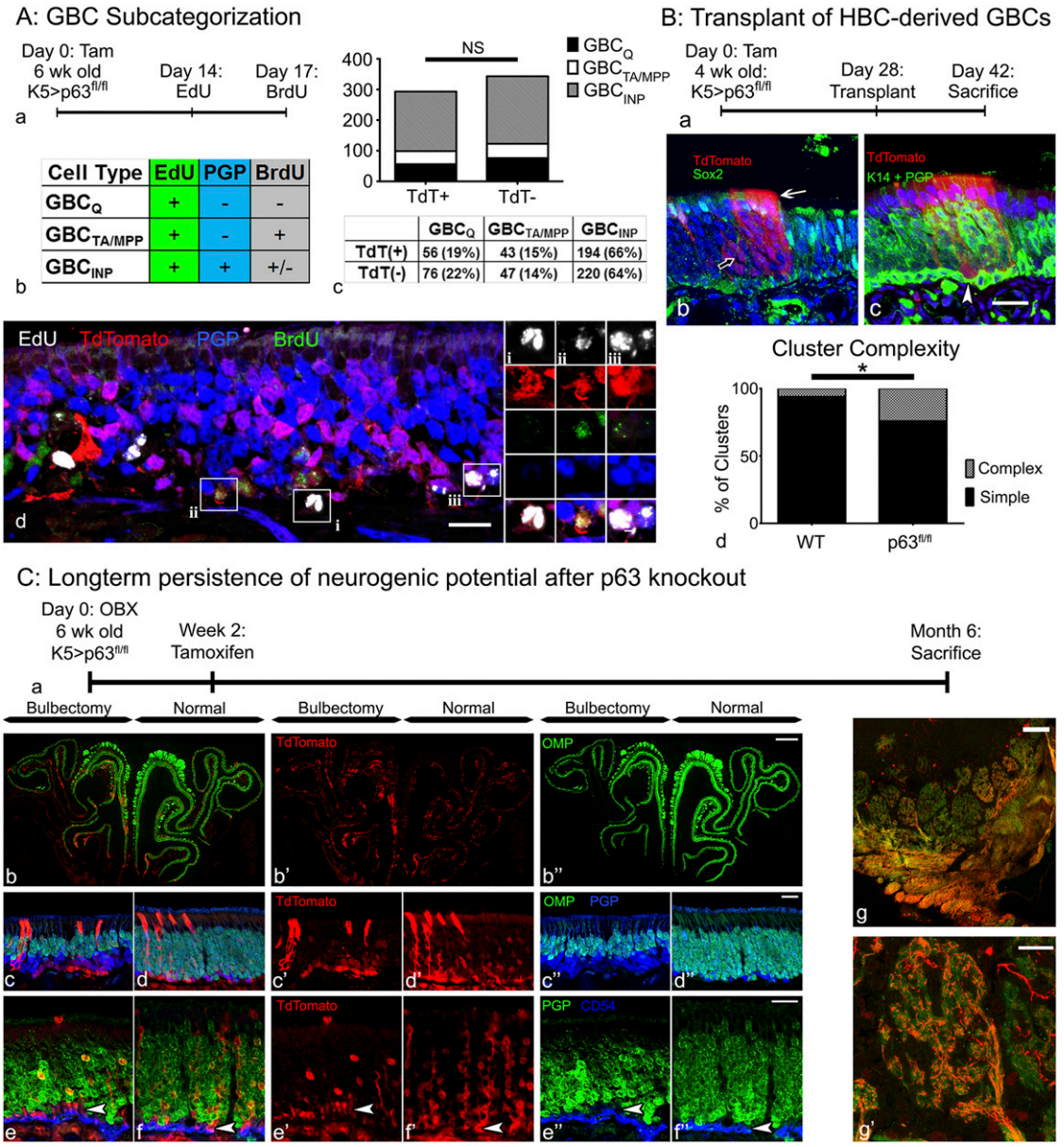

Fig. 5. Activated HBCs generate GBCs, which integrate into the tissue and retain stem cell potential comparable to endogenous GBCs. (*A*) GBC subcategorization: analysis of the proliferation dynamics of endogenous TdTomato$^-$ (TdT$^-$), and HBC-derived TdTomato$^+$ (TdT$^+$) GBCs. (*a* and *b*) Timeline (*a*) and experimental design (*b*) for assessing the different GBC subtypes in *K5.CreER^{T2} > p63$^{fl/fl}$;R26R(TdT)* animals as described in the table. Note that the population of GBC$_{INP}$s is defined by their differentiation into PGP$^+$ sensory neurons. (*c*) Quantification and comparison of TdT$^+$ (i.e., HBC-derived) and TdT$^-$ GBCs, showing no significant (NS) difference between these two GBC populations in terms of subtype distribution. (*d*) Representative section (included in the quantitative analysis in *c*) containing each of the three classifications of GBCs: (*i*) GBC$_Q$s: TdT$^+$/EdU$^+$/BrdU$^-$/PGP$^-$; (*ii*) GBC$_{TA/MPP}$s: TdT$^+$/EdU$^+$/BrdU$^+$/PGP$^-$; (*iii*) GBC$_{INP}$s: TdT$^+$/EdU$^+$/PGP$^+$. (Scale bars: 10 μm in *A*, *d*; 2 μm in *A*, *d*, *i–iii*;) (*B*) Transplantation of HBC-derived cells: Transplantation of cells from *K5.CreER^{T2} > p63$^{fl/fl}$;R26R(TdT)* mice [K*p63$^{fl/fl}$*T] 4 wk after tamoxifen injection; note that the tamoxifen-treated donor animals were unlesioned at the time of harvest. (*a*) Timeline of experimental design. (*b*) An example of a complex clone consisting of morphologically distinct OSNs (open arrow) and Sox2$^+$ Sus cells (white arrow). (*c*) An example of a complex clone containing a row of labeled Sus cells (arrow) and K14$^-$/PGP$^-$ GBCs (white arrowhead). (Scale bar: 10 μm in *B*, *b* and *c*.) (*d*) Quantification of HBC-derived clones from K*p63$^{fl/fl}$*T donors vs. WT controls (i.e., tamoxifen-treated K*p63$^{+/+}$*T from Fig. 1). *$P < 0.05$; χ^2 with Yates' correction, performed on raw data. (*C*) Long-term persistence of neurogenic potential after *p63* knockout: Analysis of HBC-derived cells in KpT animals 6 mo after OBX. (*a*) Timeline of experimental design. (*b–d*) Mosaic image encompassing the whole section (*b*) and representative high-magnification images (*c* and *d*) of KpT tissue 6 mo after OBX demonstrating significant thinning of the OMP$^+$ neuronal layer on the bulbectomized side (*c*) compared with the unoperated contralateral control side (*d*). HBC-derived TdTomato$^+$ GBCs remain neurogenic and make a substantial contribution to the population of PGP9.5$^+$ sensory neurons. (*e* and *f*) Representative high-magnification images from the bulbectomized side (*e*) and the unoperated contralateral control side (*f*) demonstrating the persistence of PGP9.5$^-$/CD54$^-$ GBCs (white arrowheads). (*g*) On the unlesioned side, TdTomato$^+$ OSNs (i.e., derived from recombined HBCs) actively contribute OMP$^+$ axons to the olfactory sensory nerve, fasciculate, and extensively innervate the olfactory bulb glomeruli (*g′*). (Scale bars: 100 μm in *C*, *b* and *g*; 20 μm in *C*, *c–f* and *g′*.)

least some GBCs generated in this manner remain multipotent, continue to cycle after the loss of p63, and do not progress into GBCs with more limited differentiative capacity and/or differentiate terminally into neurons. Thus, HBC-derived GBCs apparently persist as stem cells capable of engraftment and multipotency over the relatively long term.

Finally, we investigated the long-term persistence of HBC-derived, functional GBC stem cells in situ and their ability to contribute to neurogenesis in a neuron-specific model of injury and repair. In this model we performed a unilateral olfactory bulbectomy (OBX) by surgically removing the olfactory bulb, which is the postsynaptic target for the OSNs (Fig. 5 *C*, *a*). It is known that the neurons depend on the presence of the olfactory bulb for trophic support, and hence the lifespan of all OSNs born after OBX is truncated at about 2 wk or less (34). The continuous loss of neurons is accompanied by a significant increase in GBC division and neuronal production, without significant concomitant HBC activation (7, 34–36). To assess whether HBC-derived GBCs are able to contribute to such ongoing neurogenesis alongside endogenous GBCs, we administered tamoxifen to *K5.CreER^{T2} > p63$^{fl/fl}$;R26R (TdTomato)* mice 2 wk after OBX, a time point after the initial wave of neuronal death. The animals were left to recover for 6 mo before analysis; as a consequence, all TdTomato$^+$ neurons on the lesioned side must have been born 5 mo or more after GBC differentiated from genetically activated HBCs. In these animals both the lesioned and unlesioned sides contain abundant TdTomato$^+$ GBCs and neurons, as well as microvillar and Sus supporting cells (Fig. 5 *C*, *b–f*). Thus, GBCs derived from activated HBCs persist for an extended time despite the significantly enhanced demand for neurogenesis when neuronal lifespan is cut short. Of note, on the unlesioned side the TdTomato$^+$ sensory neurons are capable of maturing into olfactory marker protein-positive (OMP$^+$) cells, which innervate glomeruli of the olfactory bulb (Fig. 5 *C*, *f*), indicating that the HBC-derived GBCs not only are multipotent and persistent but also contribute to the maintenance of tissue and generate mature OSNs that reach their postsynaptic target.

Discussion

Our findings illustrate the contextual requirements for the activation vs. a return to quiescence of a population of reserve stem cells in the intact and regenerating OE. We have shown that activation of HBCs can be tested efficiently by transplantation into lesioned hosts. Using this approach, we were able to demonstrate that HBC activation correlates with p63 down-regulation and anticipates enhanced mitotic cycling. Down-regulation of p63 is necessary and sufficient for the activation of dormant HBCs. However, HBC activation does not necessarily lead to a global loss of stem cell capacity, because GBCs derived from HBCs are functionally similar to endogenous GBCs, retain engraftment and multipotency potential, and remain capable of ongoing neurogenesis for 5 mo or more even in the face of accelerated production of OSNs postbulbectomy. Taken together, the data indicate that *p63* is a master regulator of the reserve status and dormancy of HBCs but is not responsible for stemness in the OE, per se.

The Role of *p63* in the Maintenance and Repair of the OE. Understanding the role of *p63* in stem cell regulation has been complicated by conflicting data from various stem cell systems and conditions. For example, in the thymus, p63 is necessary to maintain the proliferative capacity of the stem cell population (37). On the other hand, in HaCaT cells (a keratinocyte-derived cell line) p63 promotes quiescence by repressing transcription of a number of positive cell-cycle regulators such as cyclin B2, *cdc2*, and topoisomerase II and activating transcription of the negative cell-cycle regulator *p57^{kip2}* (38, 39). These data underscore the context-dependency of p63 function.

Our study in the OE defines the contexts in which p63 is associated with cell proliferation vs. quiescence in this tissue. The data presented here uncouple the p63-dependent process of functional activation from the proliferation of activated cells and fit with previous data in which HBC proliferation is elicited apparently independent of activation (40, 41) and other results demonstrating the proliferation of K5/K14$^+$ basal cells in respiratory epithelium (42). Our finding that retroviral-driven expression of *p63* attenuates clone size and maintains the low mitotic index of mature, p63$^+$ HBCs suggests that p63 exerts a net inhibitory effect on the proliferation of these reserve stem cells. Nevertheless, this net negative effect is not absolute, as demonstrated here by the finding that the p63$^+$ cells actively cycle early in the regeneration of the lesioned OE.

The observation that p63 down-regulation and HBC activation occur only in response to severe and direct injury to the OE and do not happen with neuronal turnover alone strongly implicates exogenous, i.e., non–cell-autonomous, mechanisms in the governance of HBC activation. The enhancement of HBC activation by a halving of *p63* gene dosage as demonstrated by analysis of the *p63$^{fl/+}$* animals suggests that the overall balance of activating and homeostatic environmental influences and their respective signaling pathways likely serves to regulate *p63* transcript and/or protein levels. A number of pathways known to be active in the OE, including Wnt, Notch, and EGF, have been shown to affect p63 expression levels in other tissues (21, 43–45). Moreover, the environment at the time of activation can direct different outcomes, because very severe injury to the OE, worse than the damage occasioned by MeBr exposure here, causes spared HBCs to give rise to metaplastic respiratory epithelium rather than regenerating GBCs and restoring the OE (46). Further elucidation of the role of activating and quiescence-maintaining pathways and more detailed analysis of HBC expression profiles with and without epithelial injury will be necessary to use these cells in regenerative applications.

General Implications for the Dynamics of Stem Cell Transitions. The existence of multiple functional classes of stem cells, whose respective contributions to epithelial homeostasis and regeneration are contextualized by epithelial status, is not unique to the OE. Such heterogeneity has been identified in diverse tissues including intestine, skin, the hematopoietic system, and the CNS (8, 47–49). In these tissues, injury above and beyond the normal cellular turnover also serves to activate the reserve stem cells. For example, in the context of the irradiated small intestine, Bmi-1$^+$ reserve cells in the +4 position of the crypts can regenerate entire villi, including the active Lgr5$^+$ stem cell population. However, in this and other cases it is not completely understood which cell-autonomous and nonautonomous mechanisms maintain the reserve phenotype or activate reserve stem cells (47–49).

Here, we demonstrate that p63 is the central hub of a cell-autonomous network that regulates HBC maintenance and activation, so that even partial down-regulation of p63, as seen in the *p63$^{fl/+}$* cells, is sufficient to promote activation. The observation that HBC activation gives rise to long-term repopulating cells of the GBC type indicates that p63 serves to maintain a reserve phenotype rather than to regulate self-renewal of a stem cell phenotype, as has been suggested previously (28). Interestingly, the role of p63 in the OE is distinct from its role in the epidermis, where p63 regulates and maintains active stem cells. Such differences likely reflect the context dependency of different cellular and molecular environments, as discussed above.

Finally, the notions that stem cell capacity is hardier and more distributed than previously suspected and that transitions between stem cell subtypes can be governed by targeting a single conserved molecule are promising for the future use of adult stem cells in regenerative medicine. Despite the inherent challenges of harnessing these molecular mechanisms, the OE provides an easily accessible source of neurocompetent stem cells, and future studies of the contexts upstream and downstream of p63 in the OE have the potential to move toward the development of cell-based regenerative therapies for neurodegenerative disease.

Materials and Methods

C57/B6, 129S1/Sv1M, *BACT.GFP*, *R26R(TdTomato)*, and *R26R(LacZ)* mice were purchased from Jackson Laboratories. *K5.CreER^{T2}* mice were generously provided by P. Chambon, Institut d'Études Avancées de l'Université de Strasbourg, Strasbourg, France and R. Reed, Johns Hopkins University, School of Medicine, Baltimore (50). Floxed *p63* mice (*p63$^{fl/fl}$*) were kindly provided by A. Mills, Cold Spring Harbor Laboratory, Cold Spring Harbor, NY (51). All animals were housed in the American Association for Laboratory Animal Care (AALAC)-accredited vivarium at Tufts University School of Medicine. All vertebrate animal protocols were approved by the Committee for the Humane Use of Animals at Tufts University School of Medicine. MeBr exposure, OBX, transplantation, retroviral infection, and immunohistochemistry were performed as previously described (6, 29, 37, 52). Primary antibodies used, their dilutions, and detection methods are listed in Table S1. Images were obtained on a Zeiss 510 confocal microscope or on a Nikon 800E epifluorescent microscope. Image analysis was performed using ImageJ. Image preparation and figure assembly were performed in Adobe Photoshop CS2. In all photographs, only balance, contrast, and evenness of the illumination were altered. For a full description of the experimental procedures and staining conditions used in this study, please see *SI Materials and Methods*.

ACKNOWLEDGMENTS. This work was supported by NIH Grants R01 DC002167 (to J.E.S.), F30 DC011241 (to N.S.), F30 DC013962 (to D.B.H.), F31 DC 014637 (to B.L.), and F31 DC014398 (to J.H.C.).

1. Iscove NN, Nawa K (1997) Hematopoietic stem cells expand during serial transplantation in vivo without apparent exhaustion. *Curr Biol* 7(10):805–808.
2. Price J, Turner D, Cepko C (1987) Lineage analysis in the vertebrate nervous system by retrovirus-mediated gene transfer. *Proc Natl Acad Sci USA* 84(1):156–160.
3. Barker N, et al. (2009) Crypt stem cells as the cells-of-origin of intestinal cancer. *Nature* 457(7229):608–611.
4. Barker N, et al. (2007) Identification of stem cells in small intestine and colon by marker gene Lgr5. *Nature* 449(7165):1003–1007.
5. Doetsch F, Caillé I, Lim DA, García-Verdugo JM, Alvarez-Buylla A (1999) Subventricular zone astrocytes are neural stem cells in the adult mammalian brain. *Cell* 97(6):703–716.
6. Chen X, Fang H, Schwob JE (2004) Multipotency of purified, transplanted globose basal cells in olfactory epithelium. *J Comp Neurol* 469(4):457–474.
7. Leung CT, Coulombe PA, Reed RR (2007) Contribution of olfactory neural stem cells to tissue maintenance and regeneration. *Nat Neurosci* 10(6):720–726.
8. Li L, Clevers H (2010) Coexistence of quiescent and active adult stem cells in mammals. *Science* 327(5965):542–545.
9. Grompe M (2012) Tissue stem cells: New tools and functional diversity. *Cell Stem Cell* 10(6):685–689.
10. Göritz C, Frisén J (2012) Neural stem cells and neurogenesis in the adult. *Cell Stem Cell* 10(6):657–659.
11. Graziadei PP, Graziadei GA (1979) Neurogenesis and neuron regeneration in the olfactory system of mammals. I. Morphological aspects of differentiation and structural organization of the olfactory sensory neurons. *J Neurocytol* 8(1):1–18.
12. Graziadei GA, Graziadei PP (1979) Neurogenesis and neuron regeneration in the olfactory system of mammals. II. Degeneration and reconstitution of the olfactory sensory neurons after axotomy. *J Neurocytol* 8(2):197–213.
13. Schwob JE (2002) Neural regeneration and the peripheral olfactory system. *Anat Rec* 269(1):33–49.
14. Schwob JE, Jang W, Holbrook EH (2012) Stem cells of the olfactory epithelium. *Neural Development and Stem Cells*, ed Rao MS (Springer Science & Business Media, New York), 3rd Ed, pp 201–222.
15. Goldstein BJ, Fang H, Youngentob SL, Schwob JE (1998) Transplantation of multipotent progenitors from the adult olfactory epithelium. *Neuroreport* 9(7):1611–1617.
16. Caggiano M, Kauer JS, Hunter DD (1994) Globose basal cells are neuronal progenitors in the olfactory epithelium: A lineage analysis using a replication-incompetent retrovirus. *Neuron* 13(2):339–352.
17. Guo Z, et al. (2010) Expression of pax6 and sox2 in adult olfactory epithelium. *J Comp Neurol* 518(21):4395–4418.
18. Manglapus GL, Youngentob SL, Schwob JE (2004) Expression patterns of basic helix-loop-helix transcription factors define subsets of olfactory progenitor cells. *J Comp Neurol* 479(2):216–233.
19. Tucker ES, et al. (2010) Proliferative and transcriptional identity of distinct classes of neural precursors in the mammalian olfactory epithelium. *Development* 137(15):2471–2481.
20. Packard A, Schnittke N, Romano RA, Sinha S, Schwob JE (2011) DeltaNp63 regulates stem cell dynamics in the mammalian olfactory epithelium. *J Neurosci* 31(24):8748–8759.
21. Holbrook EH, Szumowski KE, Schwob JE (1995) An immunochemical, ultrastructural, and developmental characterization of the horizontal basal cells of rat olfactory epithelium. *J Comp Neurol* 363(1):129–146.
22. Mills AA, et al. (1999) p63 is a p53 homologue required for limb and epidermal morphogenesis. *Nature* 398(6729):708–713.
23. Yang A, et al. (1999) p63 is essential for regenerative proliferation in limb, craniofacial and epithelial development. *Nature* 398(6729):714–718.
24. Carroll DK, et al. (2006) p63 regulates an adhesion programme and cell survival in epithelial cells. *Nat Cell Biol* 8(6):551–561.
25. Keyes WM, et al. (2005) p63 deficiency activates a program of cellular senescence and leads to accelerated aging. *Genes Dev* 19(17):1986–1999.
26. King KE, et al. (2003) deltaNp63alpha functions as both a positive and a negative transcriptional regulator and blocks in vitro differentiation of murine keratinocytes. *Oncogene* 22(23):3635–3644.
27. Crum CP, McKeon FD (2010) p63 in epithelial survival, germ cell surveillance, and neoplasia. *Annu Rev Pathol* 5:349–371.
28. Fletcher RB, et al. (2011) p63 regulates olfactory stem cell self-renewal and differentiation. *Neuron* 72(5):748–759.
29. Packard A, Giel-Moloney M, Leiter A, Schwob JE (2011) Progenitor cell capacity of NeuroD1-expressing globose basal cells in the mouse olfactory epithelium. *J Comp Neurol* 519(17):3580–3596.
30. Huard JM, Youngentob SL, Goldstein BJ, Luskin MB, Schwob JE (1998) Adult olfactory epithelium contains multipotent progenitors that give rise to neurons and non-neural cells. *J Comp Neurol* 400(4):469–486.
31. Cau E, Gradwohl G, Fode C, Guillemot F (1997) Mash1 activates a cascade of bHLH regulators in olfactory neuron progenitors. *Development* 124(8):1611–1621.
32. Cau E, Casarosa S, Guillemot F (2002) Mash1 and Ngn1 control distinct steps of determination and differentiation in the olfactory sensory neuron lineage. *Development* 129(8):1871–1880.
33. Jang W, Chen X, Flis D, Harris M, Schwob JE (2014) Label-retaining, quiescent globose basal cells are found in the olfactory epithelium. *J Comp Neurol* 522(4):731–749.
34. Schwob JE, Szumowski KE, Stasky AA (1992) Olfactory sensory neurons are trophically dependent on the olfactory bulb for their prolonged survival. *J Neurosci* 12(10):3896–3919.
35. Schwartz Levey M, Chikaraishi DM, Kauer JS (1991) Characterization of potential precursor populations in the mouse olfactory epithelium using immunocytochemistry and autoradiography. *J Neurosci* 11(11):3556–3564.
36. Carr VM, Farbman AI (1992) Ablation of the olfactory bulb up-regulates the rate of neurogenesis and induces precocious cell death in olfactory epithelium. *Exp Neurol* 115(1):55–59.
37. Senoo M, Pinto F, Crum CP, McKeon F (2007) p63 Is essential for the proliferative potential of stem cells in stratified epithelia. *Cell* 129(3):523–536.
38. Testoni B, Mantovani R (2006) Mechanisms of transcriptional repression of cell-cycle G2/M promoters by p63. *Nucleic Acids Res* 34(3):928–938.
39. Beretta C, Chiarelli A, Testoni B, Mantovani R, Guerrini L (2005) Regulation of the cyclin-dependent kinase inhibitor p57Kip2 expression by p63. *Cell Cycle* 4(11):1625–1631.
40. Farbman AI, Ezeh PI (2000) TGF-alpha and olfactory marker protein enhance mitosis in rat olfactory epithelium in vivo. *Neuroreport* 11(16):3655–3658.
41. Getchell TV, Narla RK, Little S, Hyde JF, Getchell ML (2000) Horizontal basal cell proliferation in the olfactory epithelium of transforming growth factor-alpha transgenic mice. *Cell Tissue Res* 299(2):185–192.
42. Yu XM, et al. (2014) Reduced growth and proliferation dynamics of nasal epithelial stem/progenitor cells in nasal polyps in vitro. *Sci Rep* 4:4619.
43. Barbieri CE, Barton CE, Pietenpol JA (2003) Delta Np63 alpha expression is regulated by the phosphoinositide 3-kinase pathway. *J Biol Chem* 278(51):51408–51414.
44. Nguyen BC, et al. (2006) Cross-regulation between Notch and p63 in keratinocyte commitment to differentiation. *Genes Dev* 20(8):1028–1042.
45. Wang F, et al. (2014) Loss of TACSTD2 contributed to squamous cell carcinoma progression through attenuating TAp63-dependent apoptosis. *Cell Death Dis* 5:e1133.
46. Xie F, Fang C, Schnittke N, Schwob JE, Ding X (2013) Mechanisms of permanent loss of olfactory receptor neurons induced by the herbicide 2,6-dichlorobenzonitrile: Effects on stem cells and noninvolvement of acute induction of the inflammatory cytokine IL-6. *Toxicol Appl Pharmacol* 272(3):598–607.
47. Tian H, et al. (2011) A reserve stem cell population in small intestine renders Lgr5-positive cells dispensable. *Nature* 478(7368):255–259.
48. Yan KS, et al. (2012) The intestinal stem cell markers Bmi1 and Lgr5 identify two functionally distinct populations. *Proc Natl Acad Sci USA* 109(2):466–471.
49. Carlén M, et al. (2009) Forebrain ependymal cells are Notch-dependent and generate neuroblasts and astrocytes after stroke. *Nat Neurosci* 12(3):259–267.
50. Indra AK, et al. (1999) Temporally-controlled site-specific mutagenesis in the basal layer of the epidermis: Comparison of the recombinase activity of the tamoxifen-inducible Cre-ER(T) and Cre-ER(T2) recombinases. *Nucleic Acids Res* 27(22):4324–4327.
51. Mills AA, Qi Y, Bradley A (2002) Conditional inactivation of p63 by Cre-mediated excision. *Genesis* 32(2):138–141.
52. Soriano P (1999) Generalized lacZ expression with the ROSA26 Cre reporter strain. *Nat Genet* 21(1):70–71.
53. Schwob JE, Youngentob SL, Mezza RC (1995) Reconstitution of the rat olfactory epithelium after methyl bromide-induced lesion. *J Comp Neurol* 359(1):15–37.
54. Nakamuta N, Kobayashi S (2007) Expression of p63 in the mouse ovary. *J Reprod Dev* 53(3):691–697.
55. Chung K, Deisseroth K (2013) CLARITY for mapping the nervous system. *Nat Methods* 10(6):508–513.

56. Tomer R, Ye L, Hsueh B, Deisseroth K (2014) Advanced CLARITY for rapid and high-resolution imaging of intact tissues. *Nat Protoc* 9(7):1682–1697.
57. Grez M, Akgün E, Hilberg F, Ostertag W (1990) Embryonic stem cell virus, a recombinant murine retrovirus with expression in embryonic stem cells. *Proc Natl Acad Sci USA* 87(23):9202–9206.
58. Carter LA, MacDonald JL, Roskams AJ (2004) Olfactory horizontal basal cells demonstrate a conserved multipotent progenitor phenotype. *J Neurosci* 24(25):5670–5683.
59. Cunha C, Hort Y, Shine J, Doyle KL (2012) Morphological and behavioural changes occur following the X-ray irradiation of the adult mouse olfactory neuroepithelium. *BMC Neurosci* 13:134–148.
60. Holbrook EH, Wu E, Curry WT, Lin DT, Schwob JE (2011) Immunohistochemical characterization of human olfactory tissue. *Laryngoscope* 121(8):1687–1701.
61. Lin W, Ezekwe EA, Jr, Zhao Z, Liman ER, Restrepo D (2008) TRPM5-expressing microvillous cells in the main olfactory epithelium. *BMC Neurosci* 9:114–127.